



Weak lensing by line-of-sight halos as the origin of flux-ratio anomalies in quadruply lensed QSOs

Kaiki Taro Inoue (KINDAI, Osaka)
Ryuichi Takahashi (Hirosaki U.)

arXiv:1207.2139

2012/07/16
Nano-Workshop at IAP

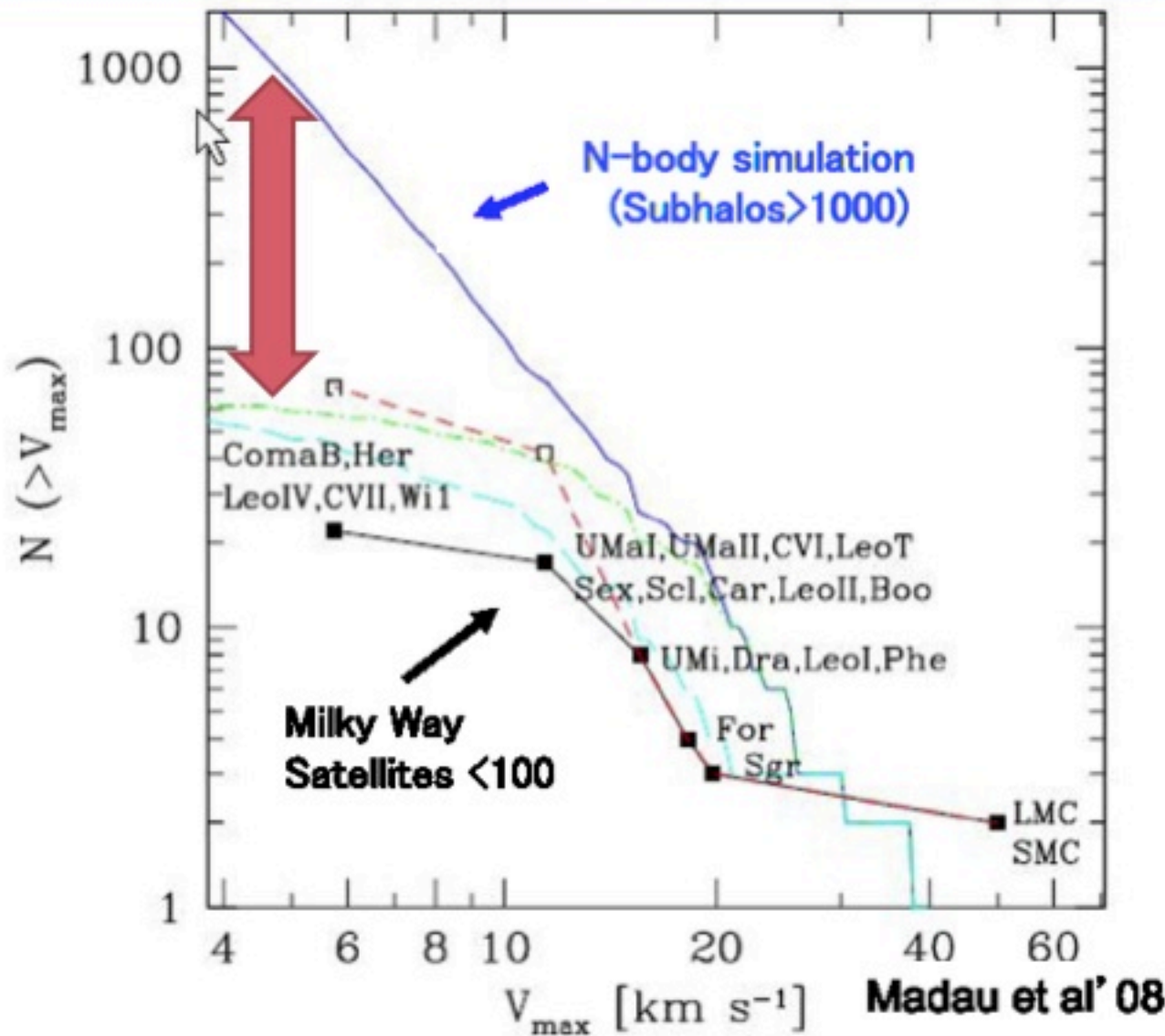


Outline

- Introduction
- Magnification perturbation
- Non-linear power spectrum
- Contribution to the flux ratios
- Summary
- Future work

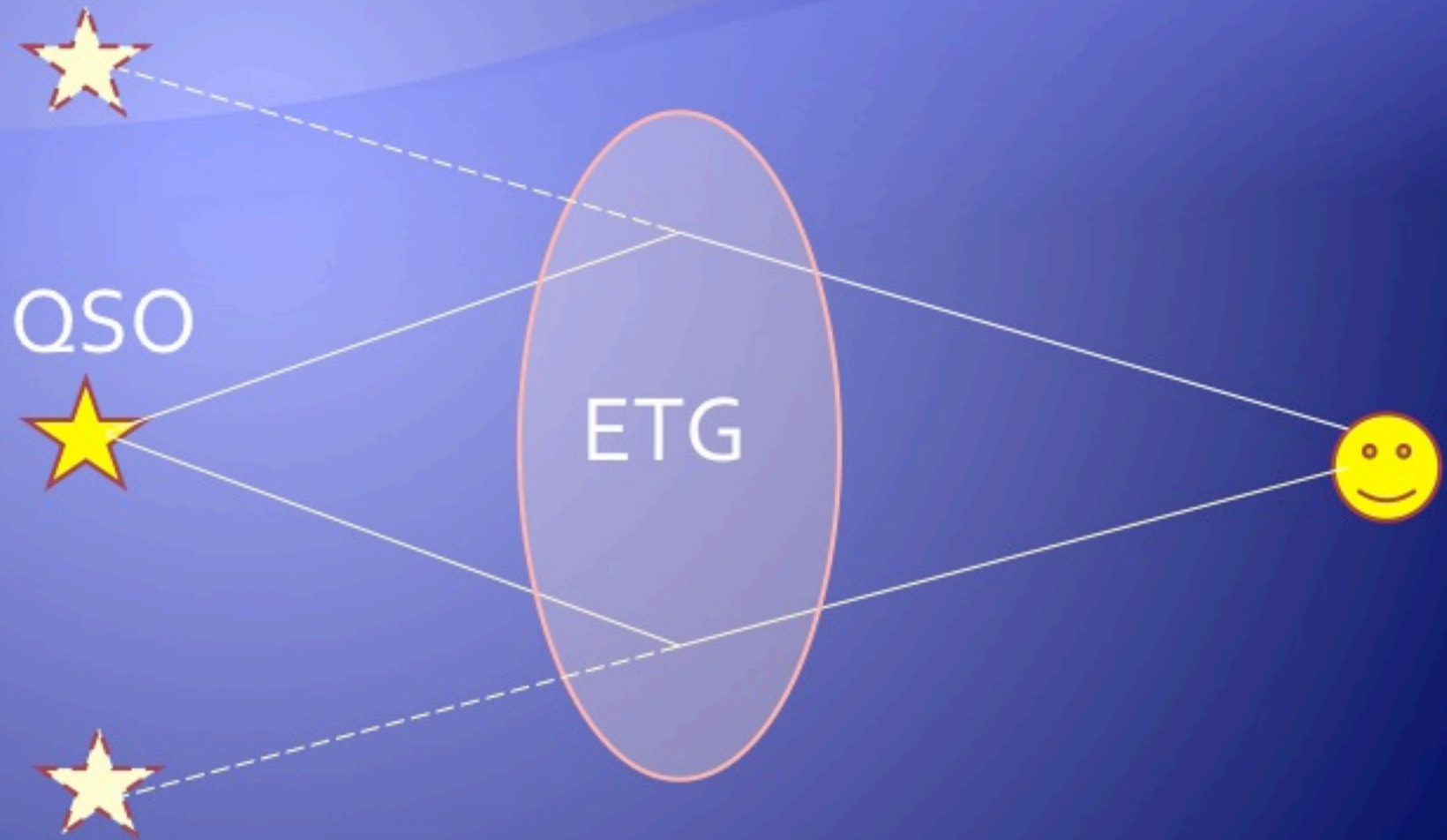
Introduction

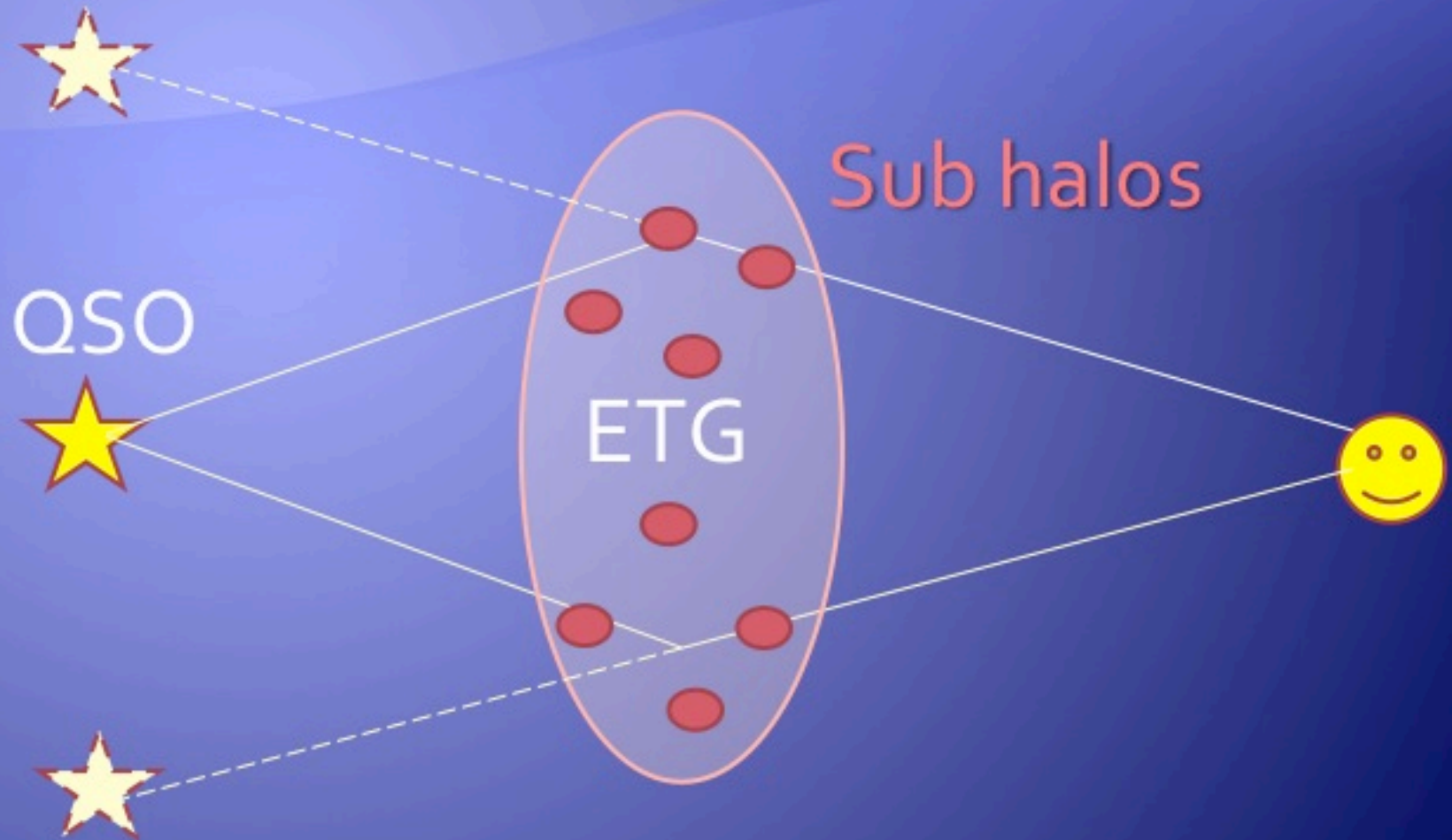
Missing Satellite Problem



Suppression Mechanism

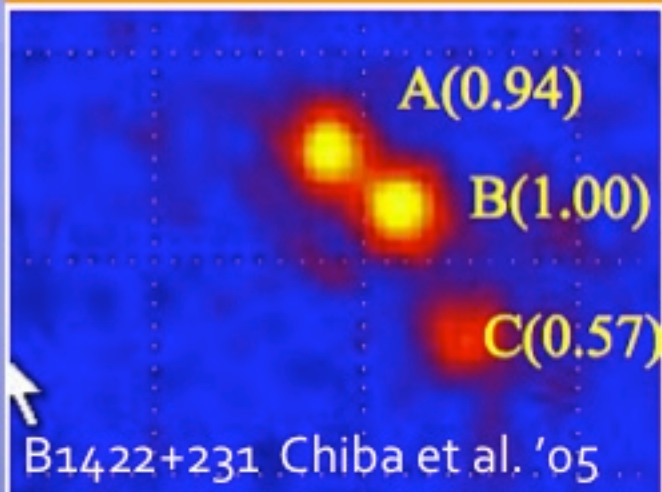
- Baryon physics (reionization, tidal disruption due to disk)
- New physics (warm dark matter, super WIMPs)
- Need to probe clustering property of halos with $M < 10^9$ solar mass





Flux- ratio anomalies

SUBARU Mid-IR image



- Positions can be well fit to the model.
- Flux-ratios fits are poor.

Cusp-caustic relation

$$\frac{A + B + C}{|A| + |B| + |C|} = 0$$

(Mao & Schneider '98
Metcalf & Madau '01,
Chiba '02 Dalal &
Kochanek '02)

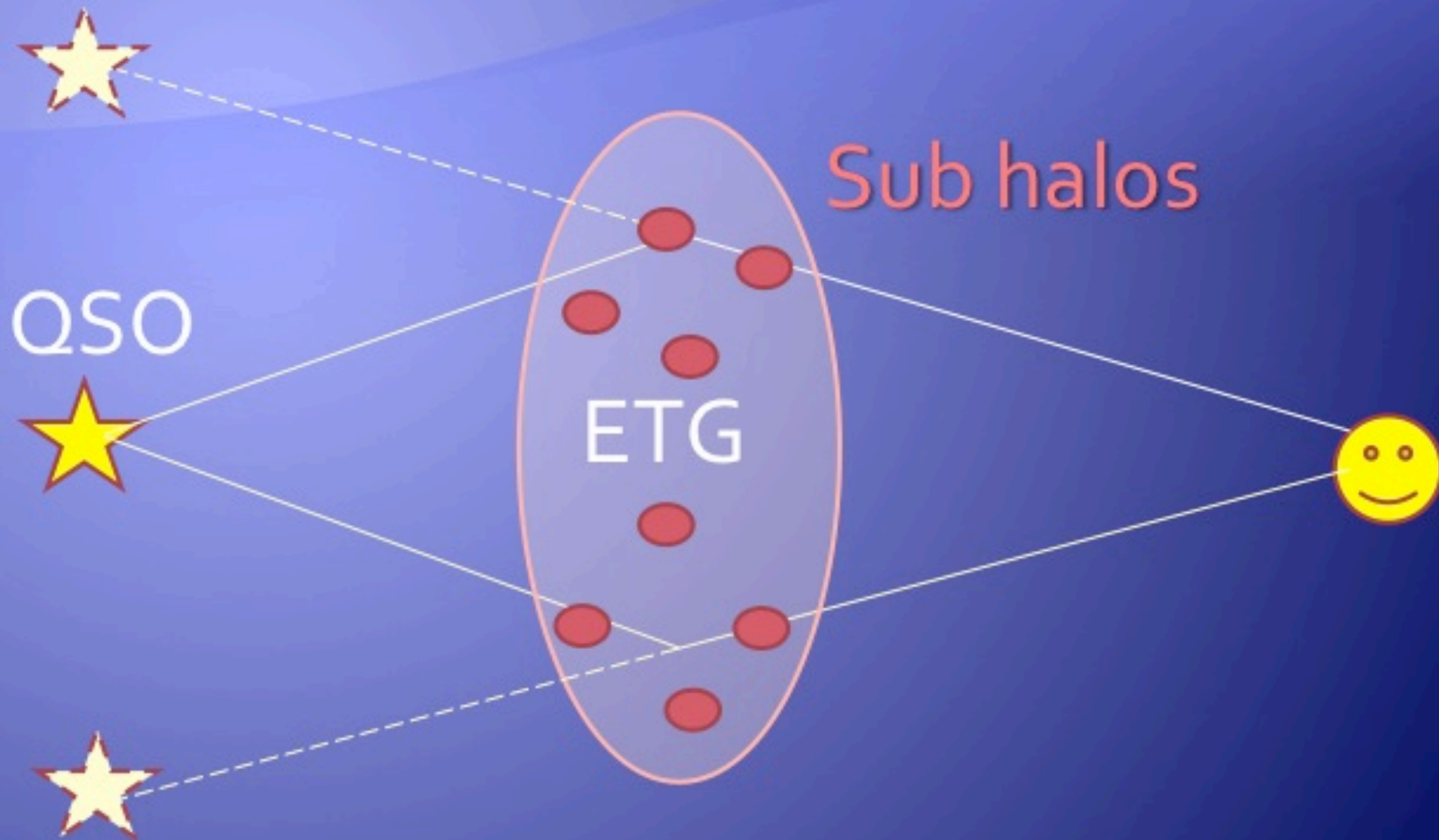
Flux- ratio anomalies

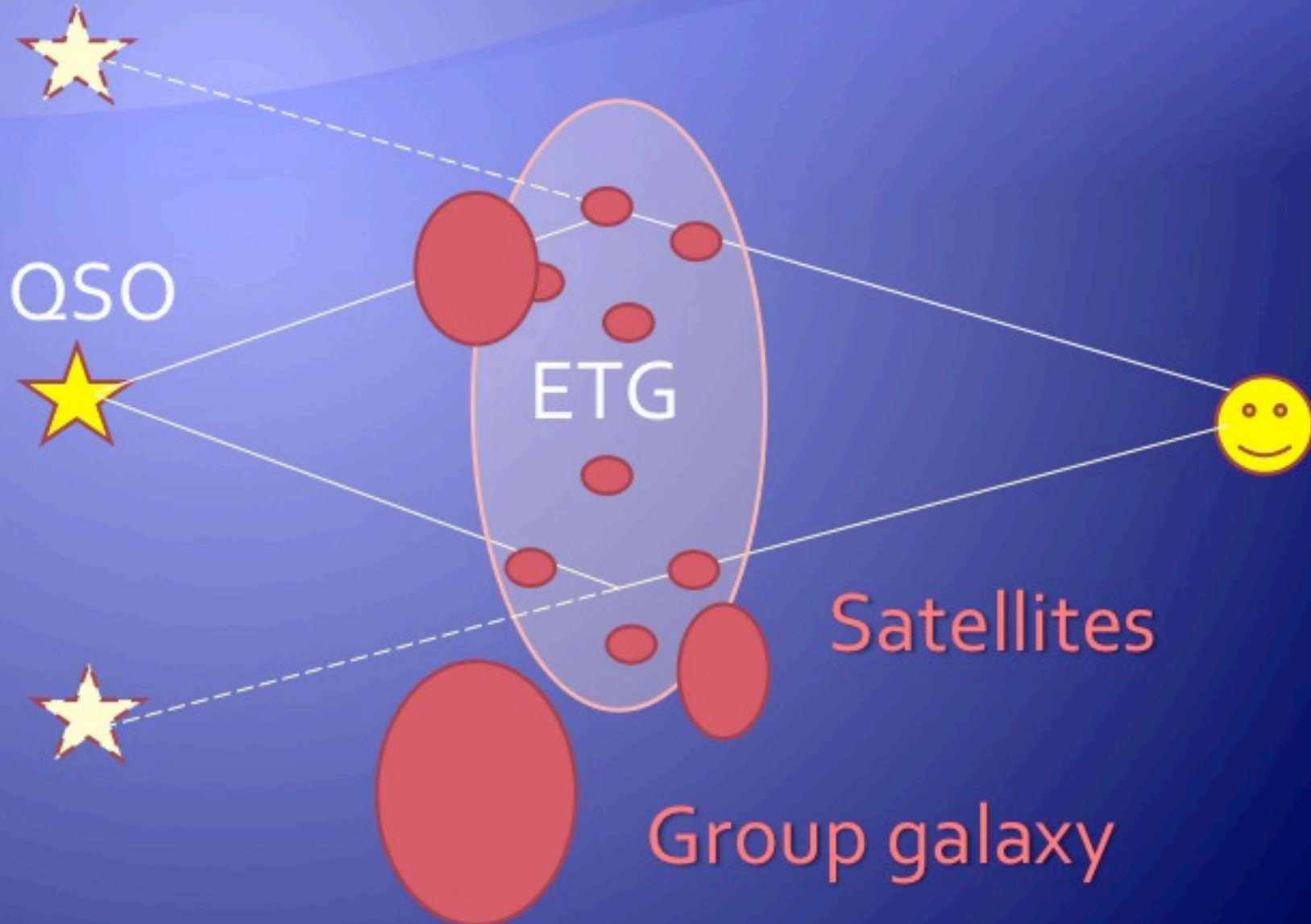
- Predicted subhalos too low for anomalies
(Maccio & Miranda 2006, Amara et al. 2006;
Xu et al. 2009, 2010; Chen 2009; Chen et al. 2011)
- Luminous satellites may contribute significantly
(McKean et al. 2007, Shin & Evans 2008;
MacLeod et al. 2009)
- Line-of-sight halos?
(Chen et al. 2003, Metcalf 2005, Xu et al. 2011)

Flux- ratio anomalies

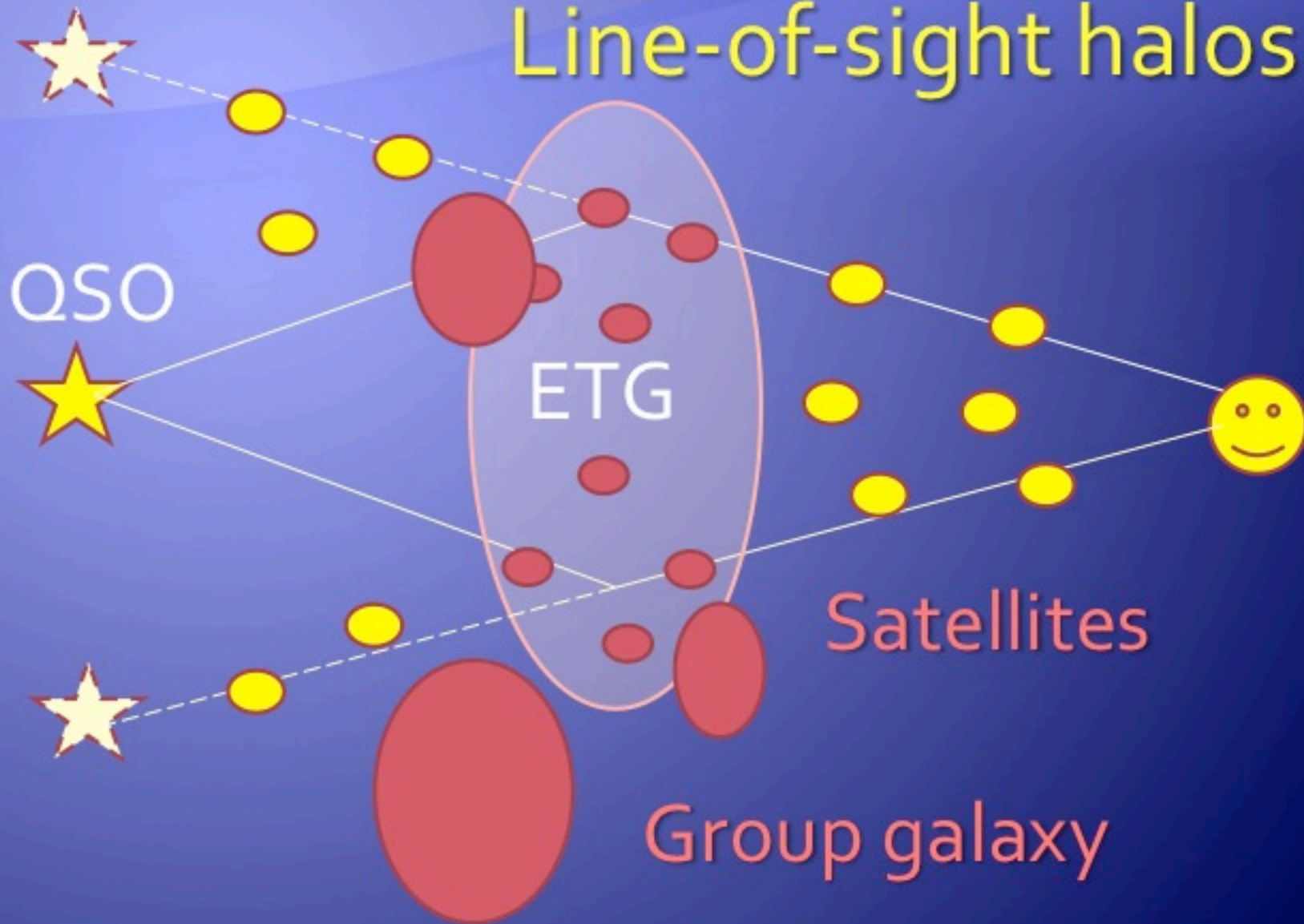
- Predicted subhalos too low for anomalies
(Maccio & Miranda 2006, Amara et al. 2006;
Xu et al. 2009, 2010; Chen 2009; Chen et al. 2011)
- Luminous satellites may contribute significantly
(McKean et al. 2007, Shin & Evans 2008;
MacLeod et al. 2009)
- Line-of-sight halos?
(Chen et al. 2003, Metcalf 2005, Xu et al. 2011)

Flux- ratio anomalies





Line-of-sight halos

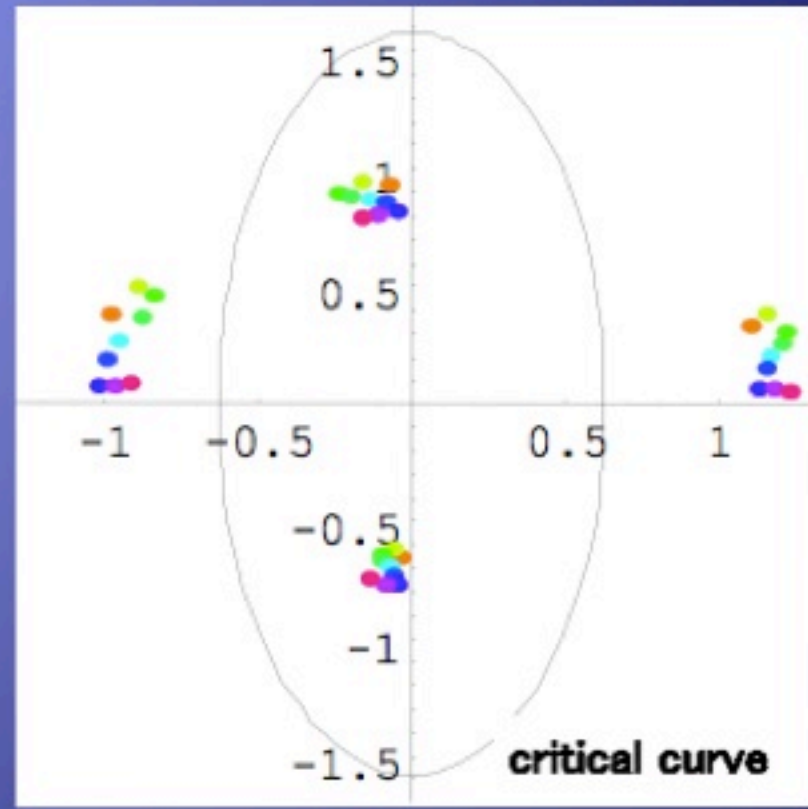
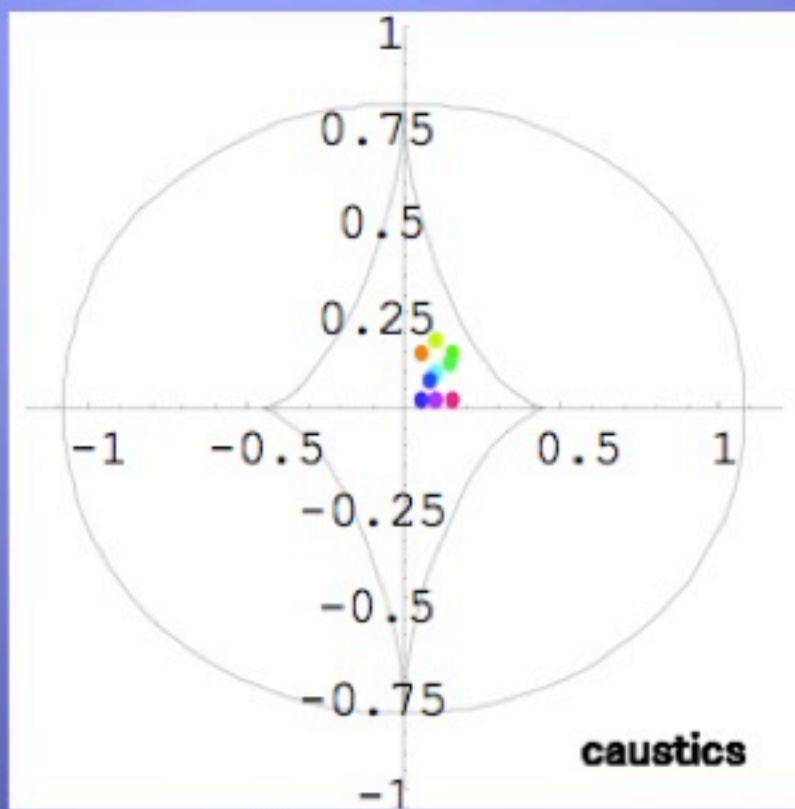


Our work

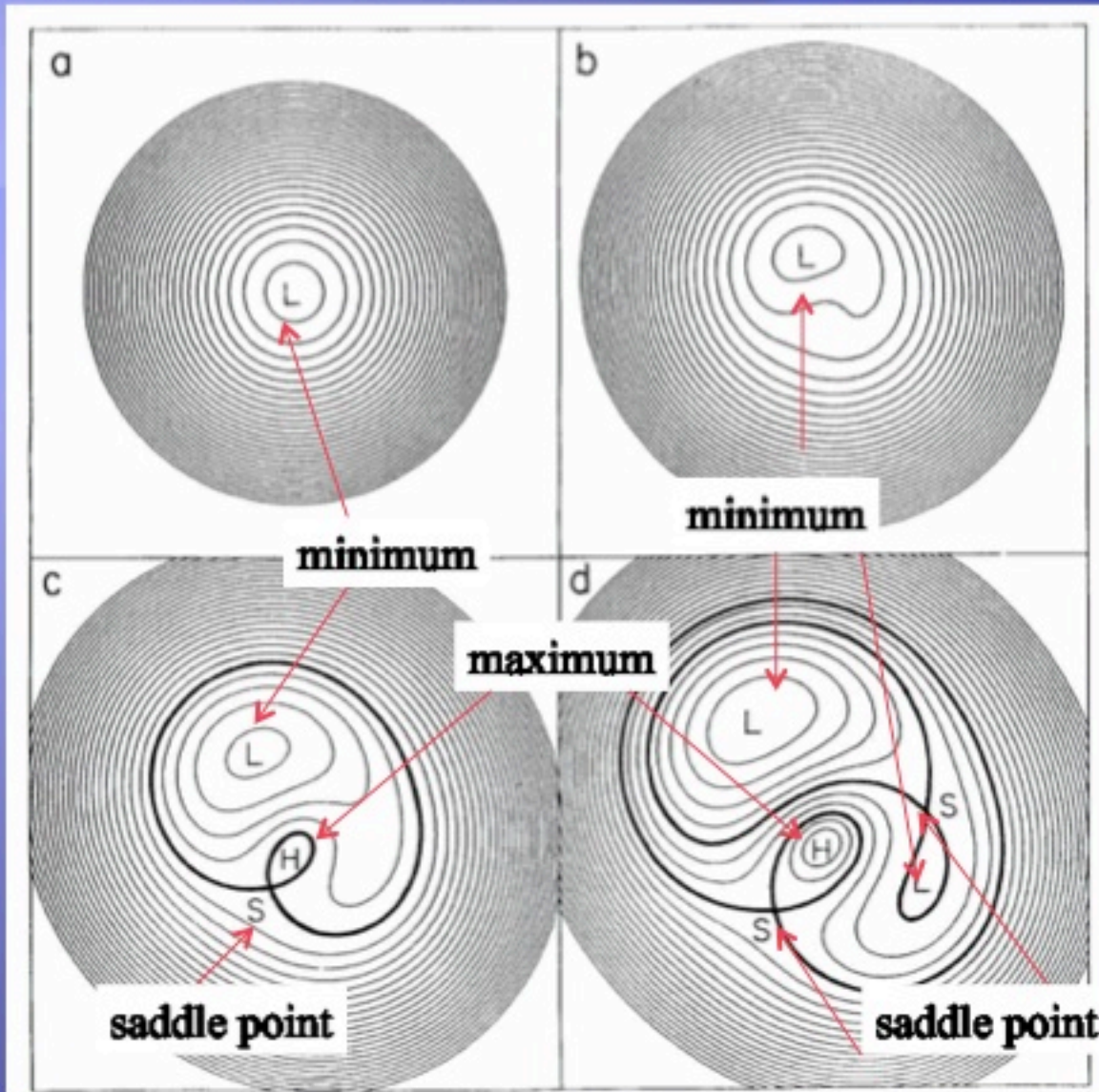
- Semi-analytic estimate based on VERY high resolution N-body simulation fully incorporating clustering effects $>10^5$ solar mass halos
- Astrometric shifts taken into account
- New static rather than 'classic' cusp-caustic relations
- Only MIR lenses. Source sizes = $O[1\text{ pc}]$

Magnification perturbation

Parity of lensed images



Arrival time surface



Systematic (de)magnification

-+



demagnify
or magnify

++



magnify

--



demagnify



or



New statistic η

A,C: minima B:saddle, $\kappa \downarrow B < 1$

$$\delta_i^\mu \equiv \delta\mu_i / \mu_i.$$
 :magnification contrast

η : effective magnification perturbation

$$\eta^2(A, B, C) = \frac{1}{4}[(\delta_A^\mu - \delta_B^\mu)^2 + (\delta_C^\mu - \delta_B^\mu)^2].$$

$$\eta^2 \approx \frac{1}{4} \left[\left(\frac{AB_0}{A_0B} - 1 \right)^2 + \left(\frac{CB_0}{C_0B} - 1 \right)^2 \right].$$

New statistic η

$$\begin{aligned}\langle \eta^2 \rangle = & \frac{1}{4} \left[(J_A + J_B) \sigma_\kappa^2(0) - 2J_{AB} \xi_\kappa(\theta_{AB}) \right. \\ & \left. + (J_B + J_C) \sigma_\kappa^2(0) - 2J_{BC} \xi_\kappa^2(\theta_{BC}) \right],\end{aligned}$$

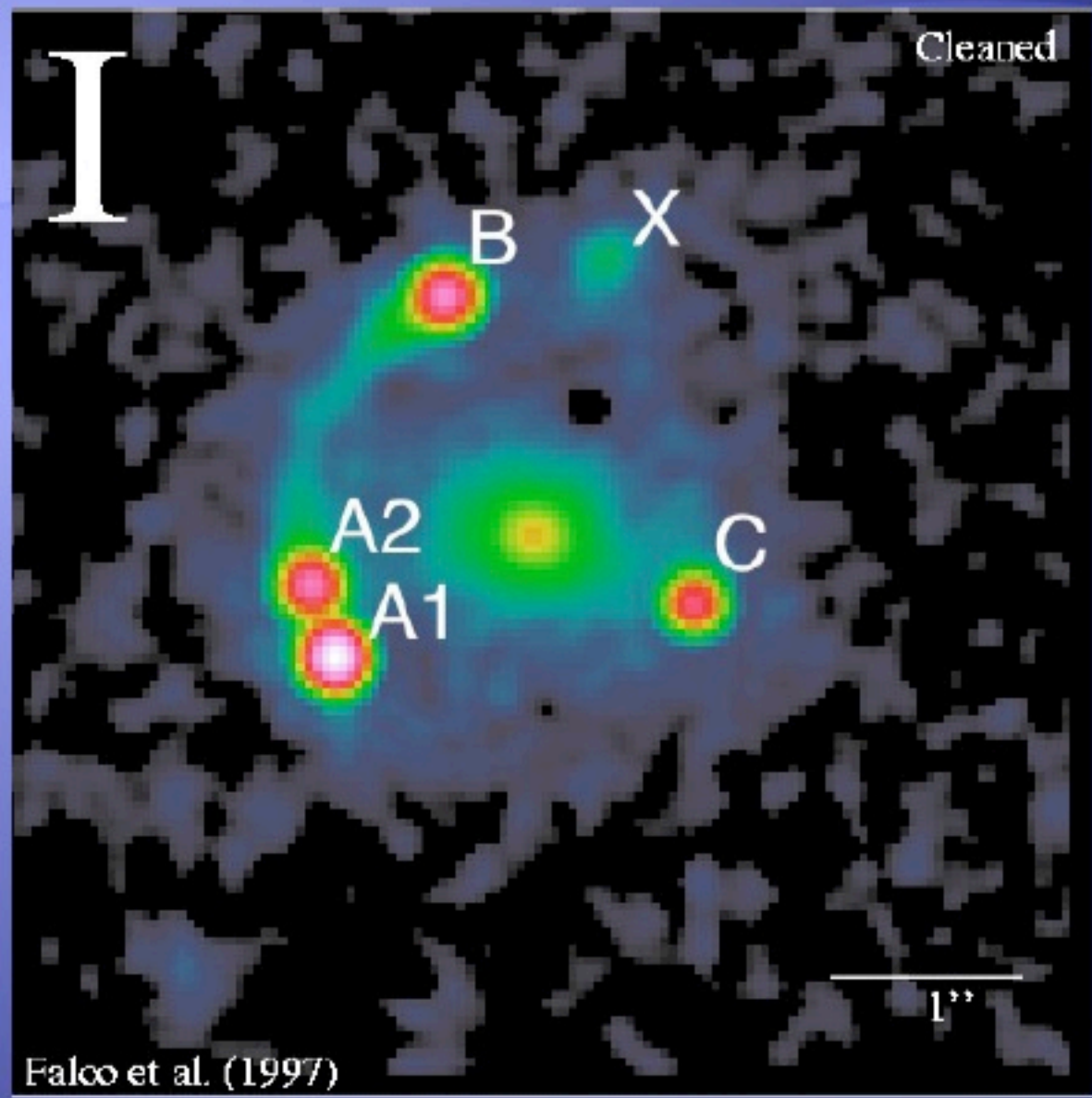
where

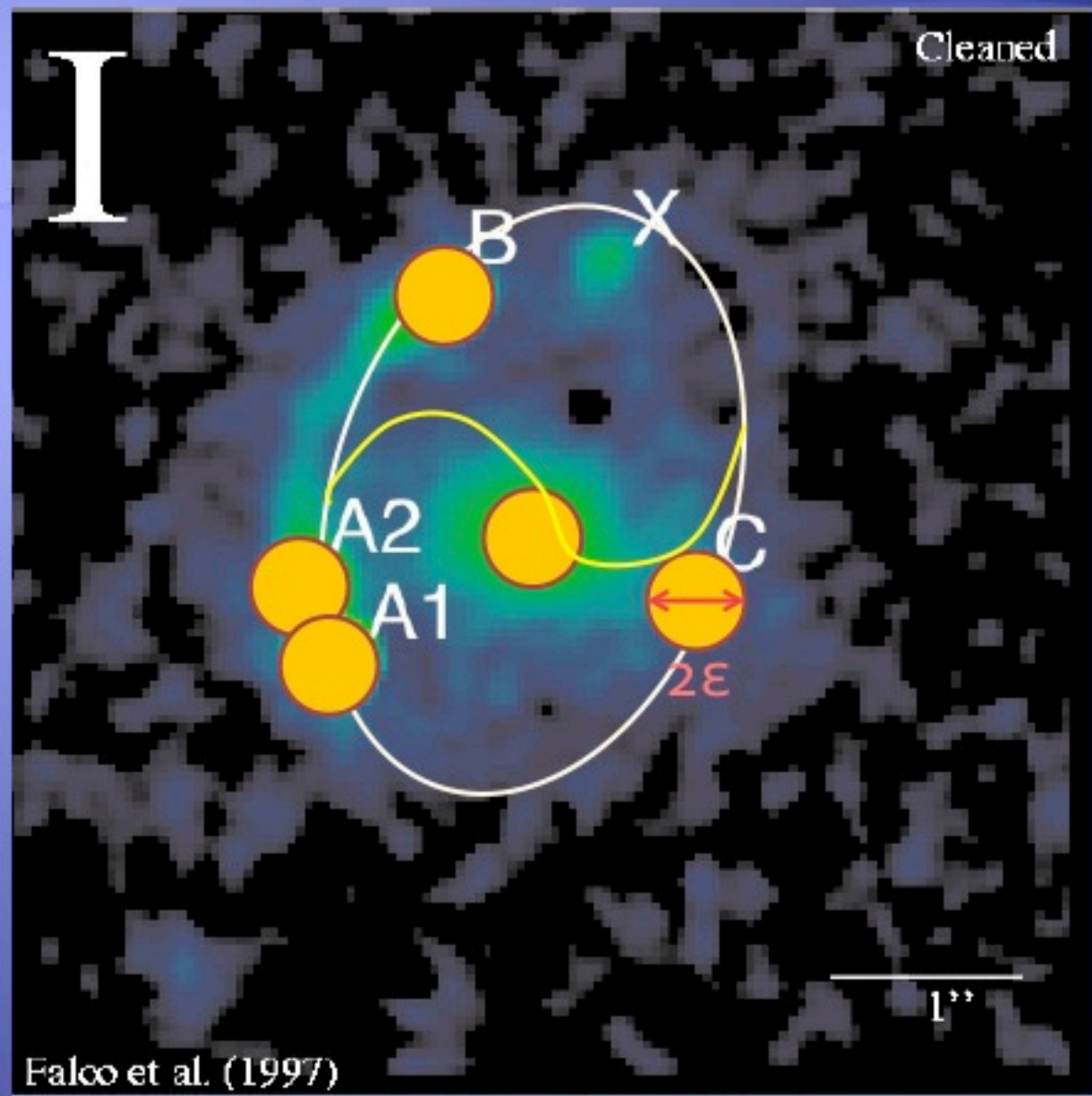
$$J_i = \mu_i^2 (4(1 - \kappa_i)^2 + 2\gamma_i^2),$$

and

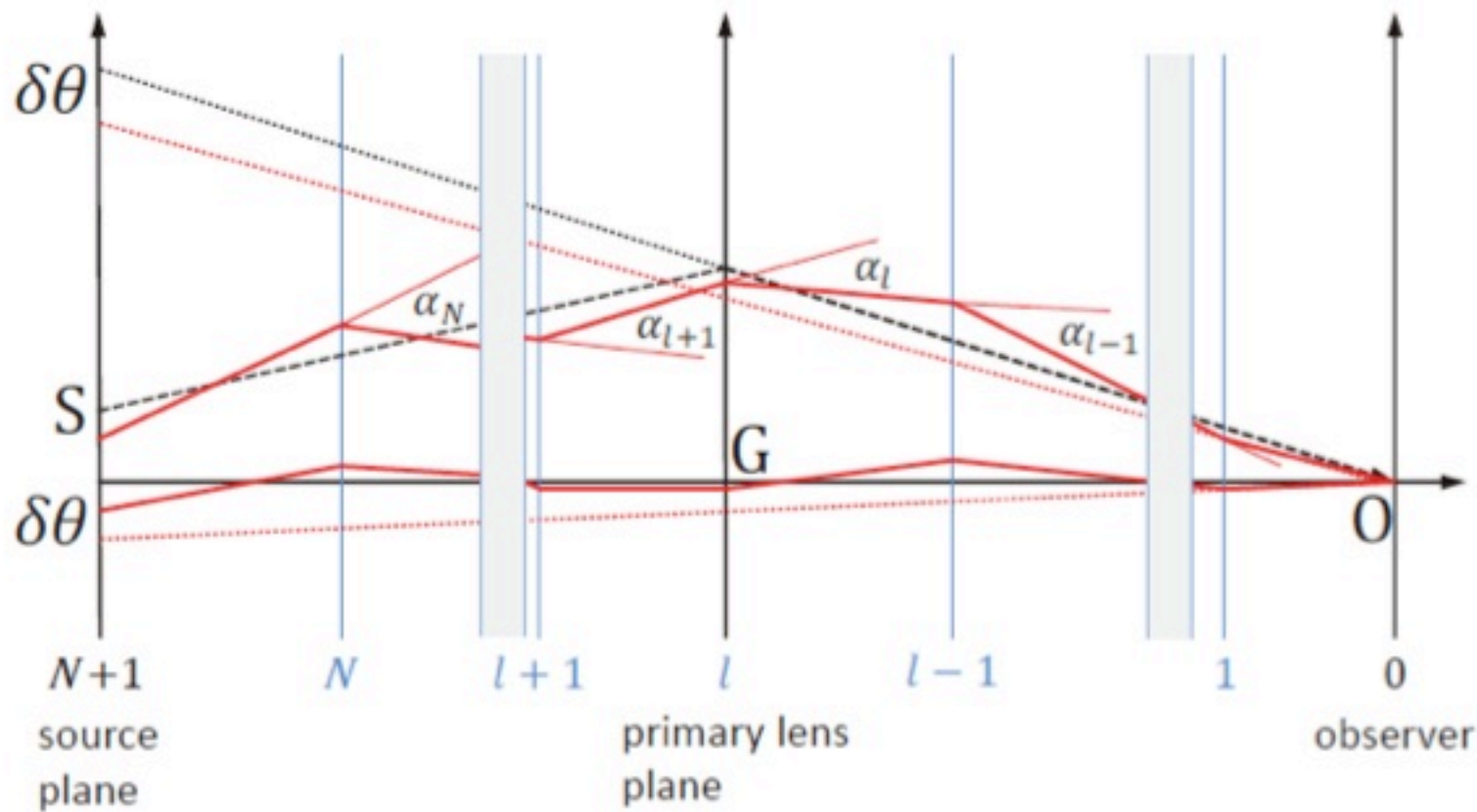
$$J_{ij} = \mu_i \mu_j (4(1 - \kappa_i)(1 - \kappa_j) + 2\gamma_i \gamma_j),$$

κ : background convergence γ : background shear





Astrometric shifts



Astrometric shifts

2-point correlation in shift of image separated by θ

$$\xi_{\delta\theta}(\theta) \equiv \langle \delta\theta(0)\delta\theta(\theta) \rangle$$

Given by power spectrum $P(k)$

$$2\langle \delta\theta^2(0) \rangle - 2\langle \delta\theta(0)\delta\theta(\theta_{AB}) \rangle < \epsilon^2,$$

Given by accuracy in position of centroid ϵ

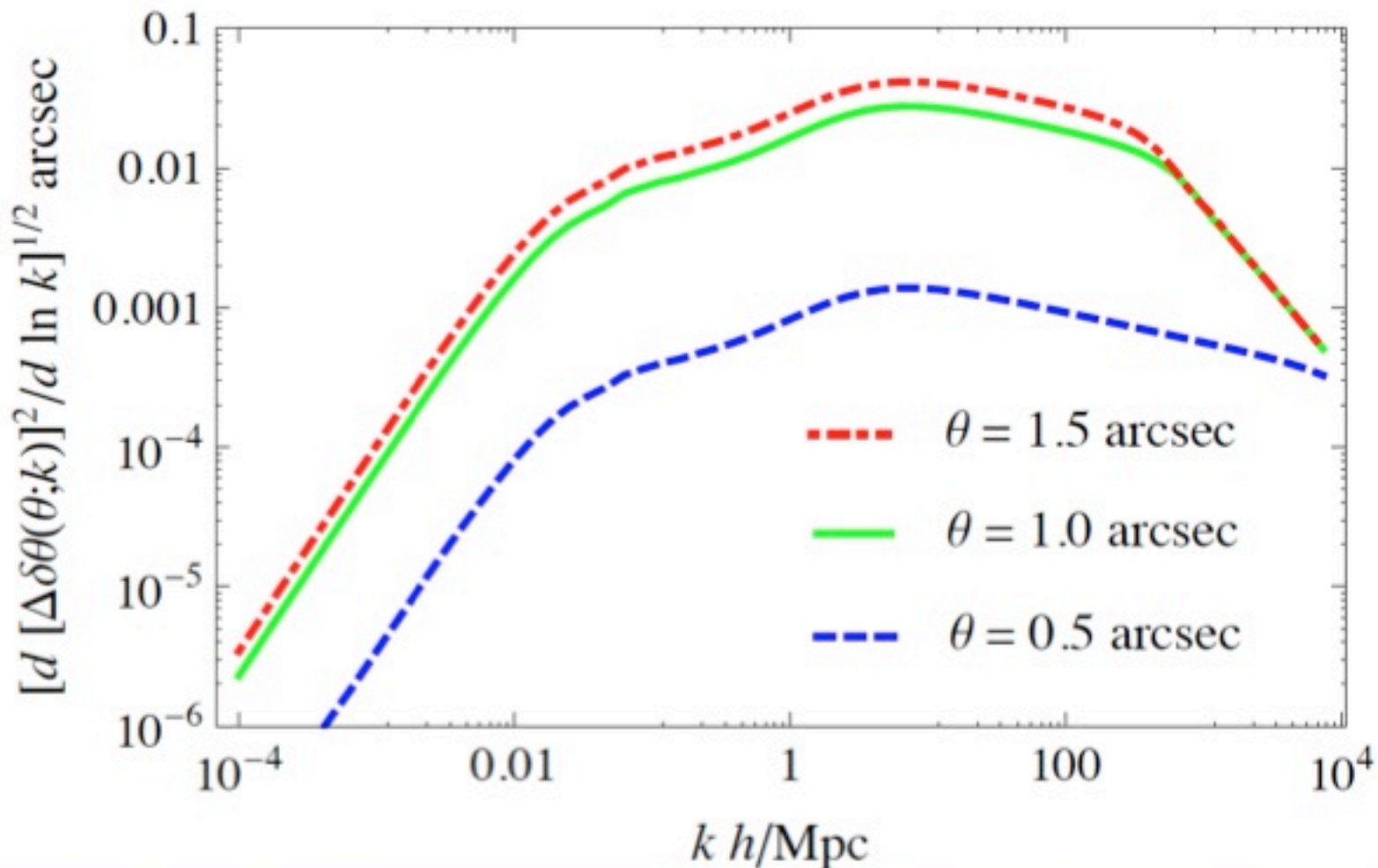
Astrometric shifts

$$k_{lens} \equiv 2\pi/L_{lens} \text{ where } L_{lens} \sim 4r(z_L)\theta_E$$

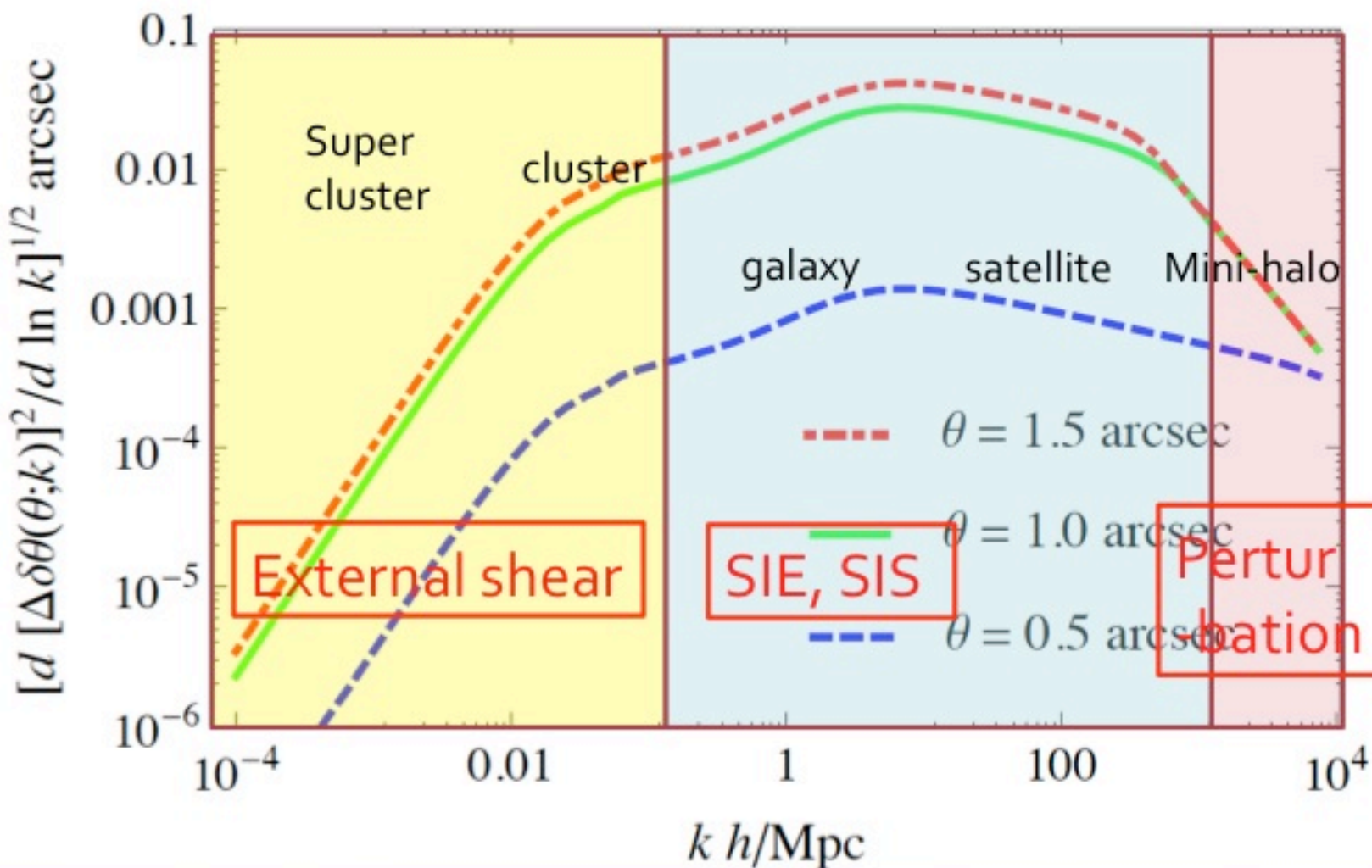
Minimum wavelength given by
the size of Einstein radius

$$k_{lens} = O[100-1000] h/\text{Mpc}$$

Astrometric shifts



Astrometric shifts



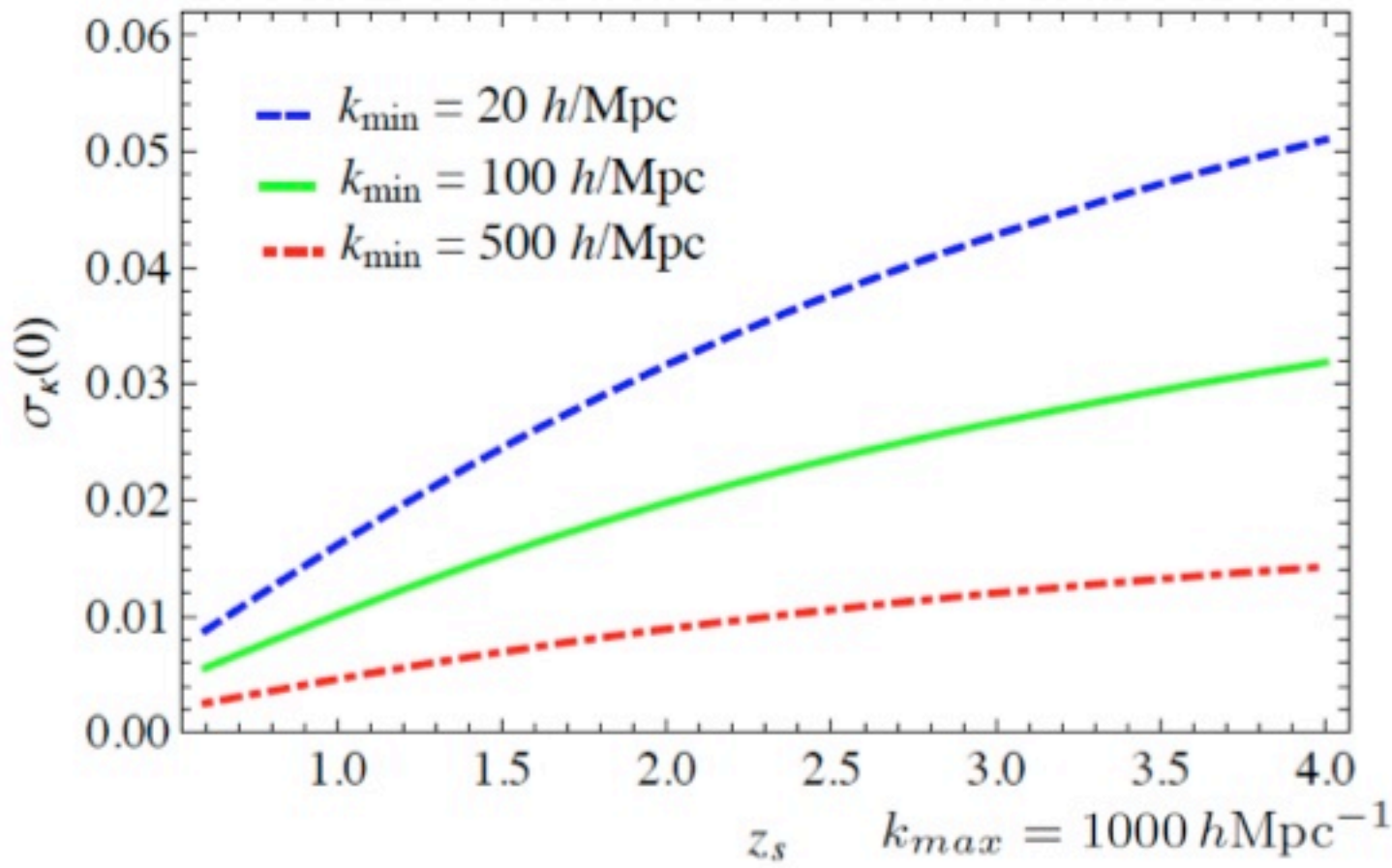
Constrained convergence power

- Accuracy in lensed images and lens = maximum contribution
- Size of the Einstein ring
(absorbed into background shear)
- These two give the largest scale of modes
 $k \downarrow min$ that can affect the flux-ratios

New statistic η

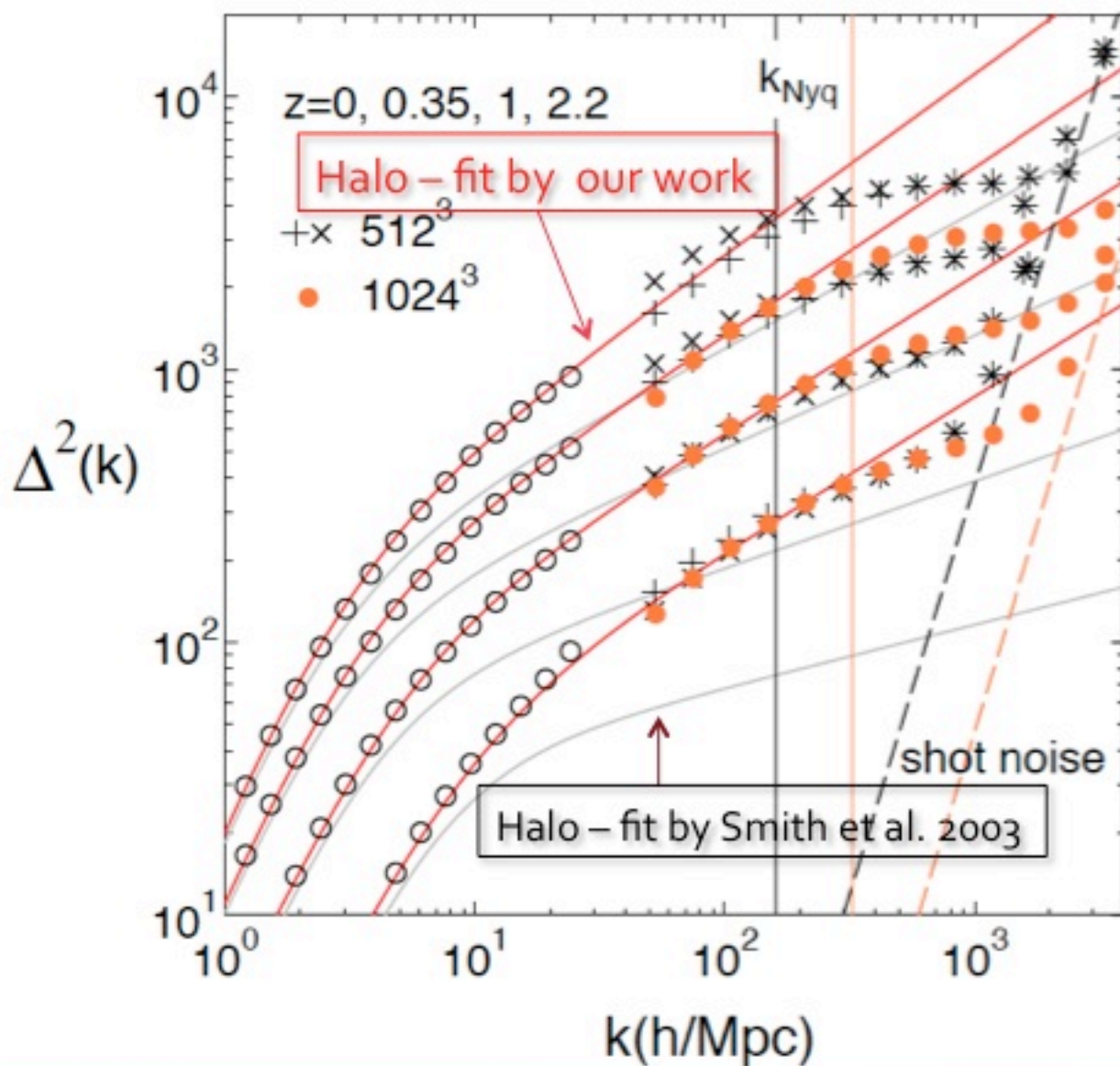
$$\begin{aligned}\xi_\kappa(\theta) &\equiv \langle \delta\kappa(0)\delta\kappa(\theta) \rangle \\ &= \frac{9H_0^4\Omega_{m,0}^2}{4c^4} \int_0^{r_S} dr r^2 \left(\frac{r - r_S}{r_S} \right)^2 [1 + z(r)]^2 \\ &\times \int_0^\infty \frac{dk}{2\pi} k \textcircled{W(k; k_{cut}(r; \epsilon))} P_\delta(k; r) J_0(g(r)k\theta),\end{aligned}$$

Constrained convergence power

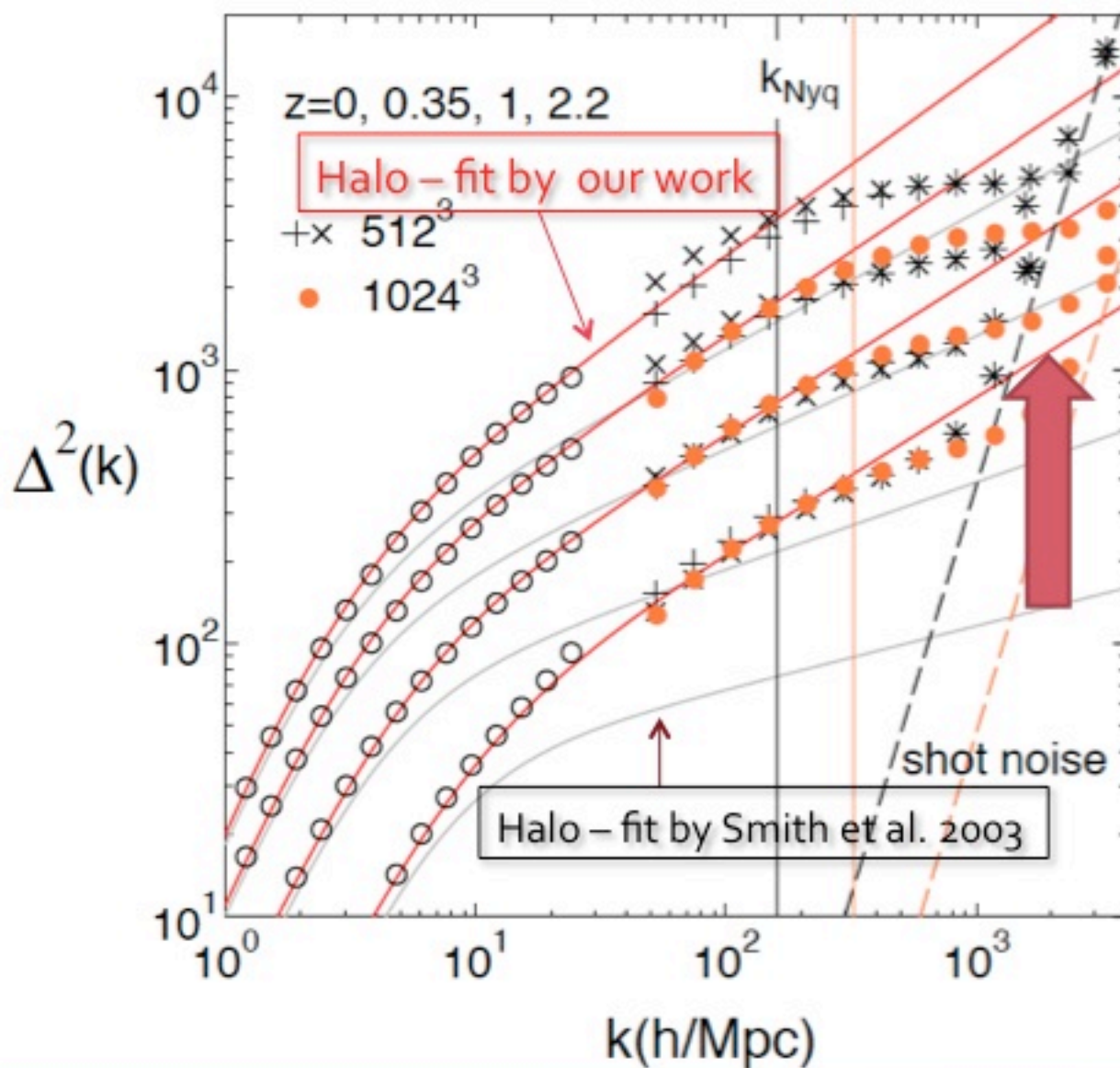


Non-linear power spectrum

Non-linear power spectrum



Non-linear power spectrum



Contribution to the flux ratios

MIR QSO-galaxy quads

- 6 samples: 5 continuum + line [OIII]
- SIE-ES model possibly with SIS for a luminous satellite (gravlens by Keeton)
- Astrometric shifts given by position errors (CASTLES) in lensed images and lens & size of critical curves -> minimum wavelength.

MIR quadruple lenses

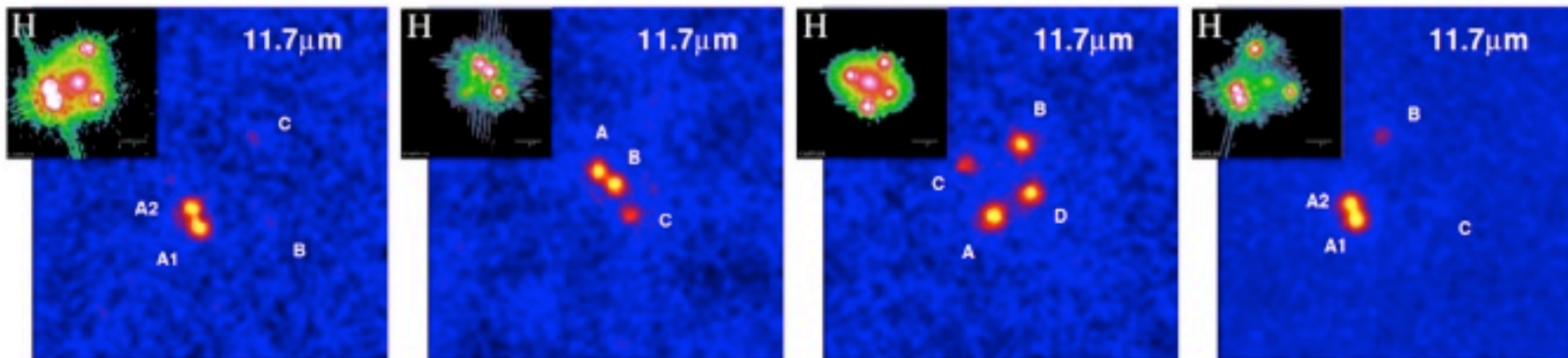


Figure 2: The mid-infrared images of quadruply lensed QSOs obtained by COMICS attached on Subaru telescope. From left to right, PG1115+080, B1422+231, Q2237+030, and MG0414+0534. The insets are their HST images for comparison (taken from CASTLES, <http://cfa-www.harvard.edu/glensdata/>).

- Source size estimated from dust reverberation method ~ 1~3pc >> Einstein radius of stars
(by Chiba et al 2005 & Minezaki et al. 2009)

MIR quadruple lenses

Table 1. Observed MIR Flux Ratios

Lens	z_L	z_S	N	Flux Ratio			$\langle \epsilon \rangle (\text{''})$	$\langle \theta \rangle (\text{''})$	Reference
RXJ1131-1231(*)				A/B 0.295 0.658 3 $1.63^{+0.04}_{-0.02}$	C/B 1.19 $^{+0.03}_{-0.12}$		0.017	1.9	1, 2
Q2237+0305	0.04	1.695	4	B/A 0.84 ± 0.05	C/A 0.46 ± 0.02	D/A 0.87 ± 0.05	0.0046	0.9	1, 3
PG1115+080	0.31	1.72	2	A2/A1 0.93 ± 0.06			0.020	1.2	1, 4
H1413+117	1.88(**)	2.55	4	B/A 0.84 ± 0.07	C/A 0.72 ± 0.07	D/A 0.40 ± 0.06	0.020	0.6	5
MG0414+0534	0.96	2.639	3	A2/A1 0.90 ± 0.04	B/A1 0.36 ± 0.02		0.0042	1.2	1, 3
B1422+231	0.34	3.62	3	A/B 0.94 ± 0.05	C/B 0.57 ± 0.06		0.0042	1.1	1, 4

References: 1. CASTLES; 2. Sugai et al. 2007; 3. Minezaki et al. 2009; 4. Chiba et al. 2005; 5. MacLeod et al. 2009

Note: (*): [OIII] line flux ratios. (**): The lens redshift z_L is obtained from a best-fit model using the observed positions of the images and the primary lens, the flux ratios, and the time-delays between the images assuming $H_0 = 70 \text{ km/s/Mpc}$.

MIR quadruple lenses

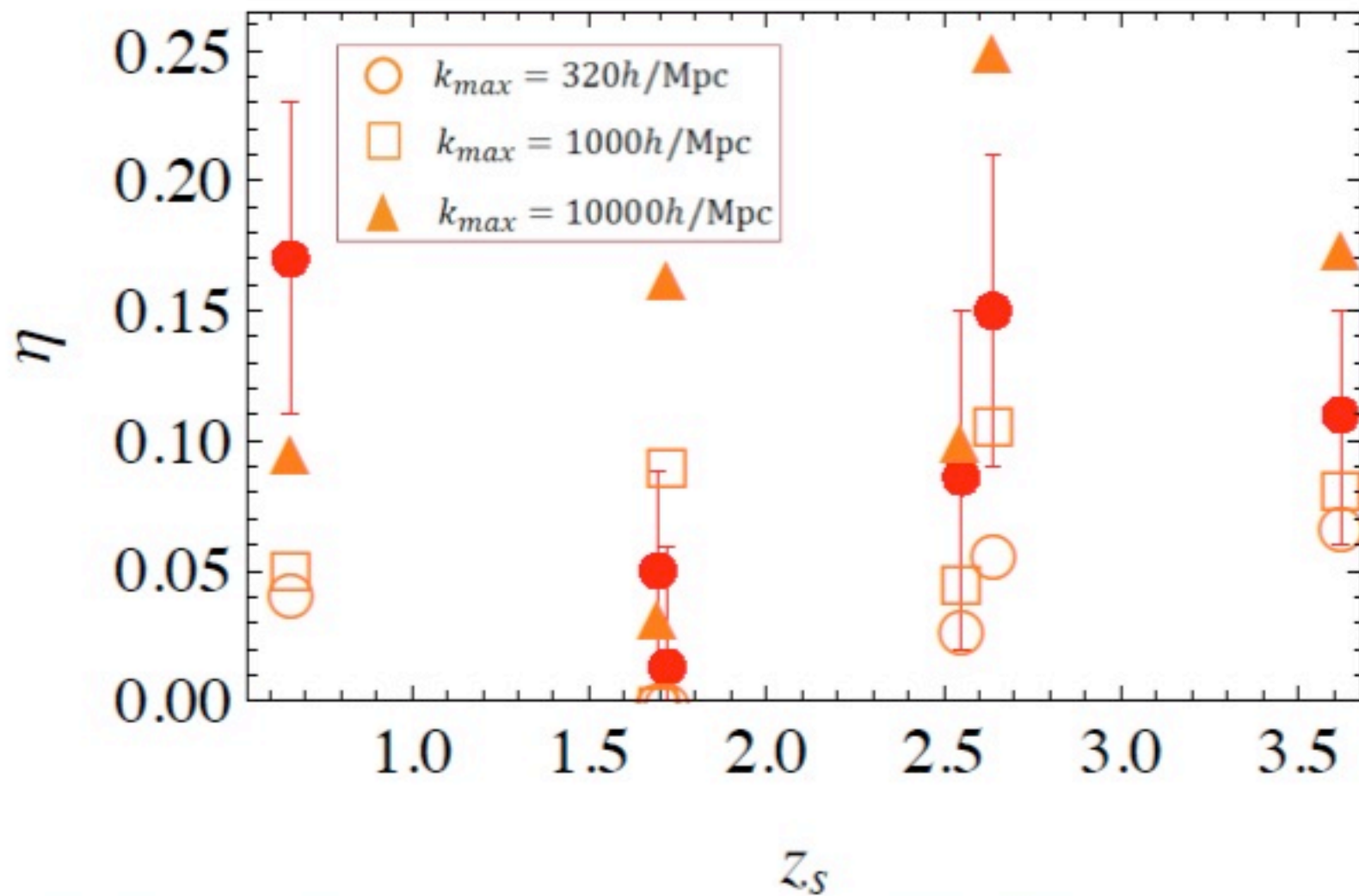
Table 1. Observed MIR Flux Ratios

Lens	z_L	z_S	N	Flux Ratio			$\langle \epsilon \rangle (\text{''})$	$\langle \theta \rangle (\text{''})$	Reference
RXJ1131-1231(*)	0.295	0.658	3	A/B $1.63^{+0.04}_{-0.02}$	C/B $1.19^{+0.03}_{-0.12}$		0.017	1.9	1, 2
Q2237+0305	0.04	1.695	4	B/A 0.84 ± 0.05	C/A 0.46 ± 0.02	D/A 0.87 ± 0.05	0.0046	0.9	1, 3
PG1115+080	0.31	1.72	2	A2/A1 0.93 ± 0.06			0.020	1.2	1, 4
H1413+117	1.88(**)	2.55	4	B/A 0.84 ± 0.07	C/A 0.72 ± 0.07	D/A 0.40 ± 0.06	0.020	0.6	5
MG0414+0534	0.96	2.639	3	A2/A1 0.90 ± 0.04	B/A1 0.36 ± 0.02		0.0042	1.2	1, 3
B1422+231	0.34	3.62	3	A/B 0.94 ± 0.05	C/B 0.57 ± 0.06		0.0042	1.1	1, 4

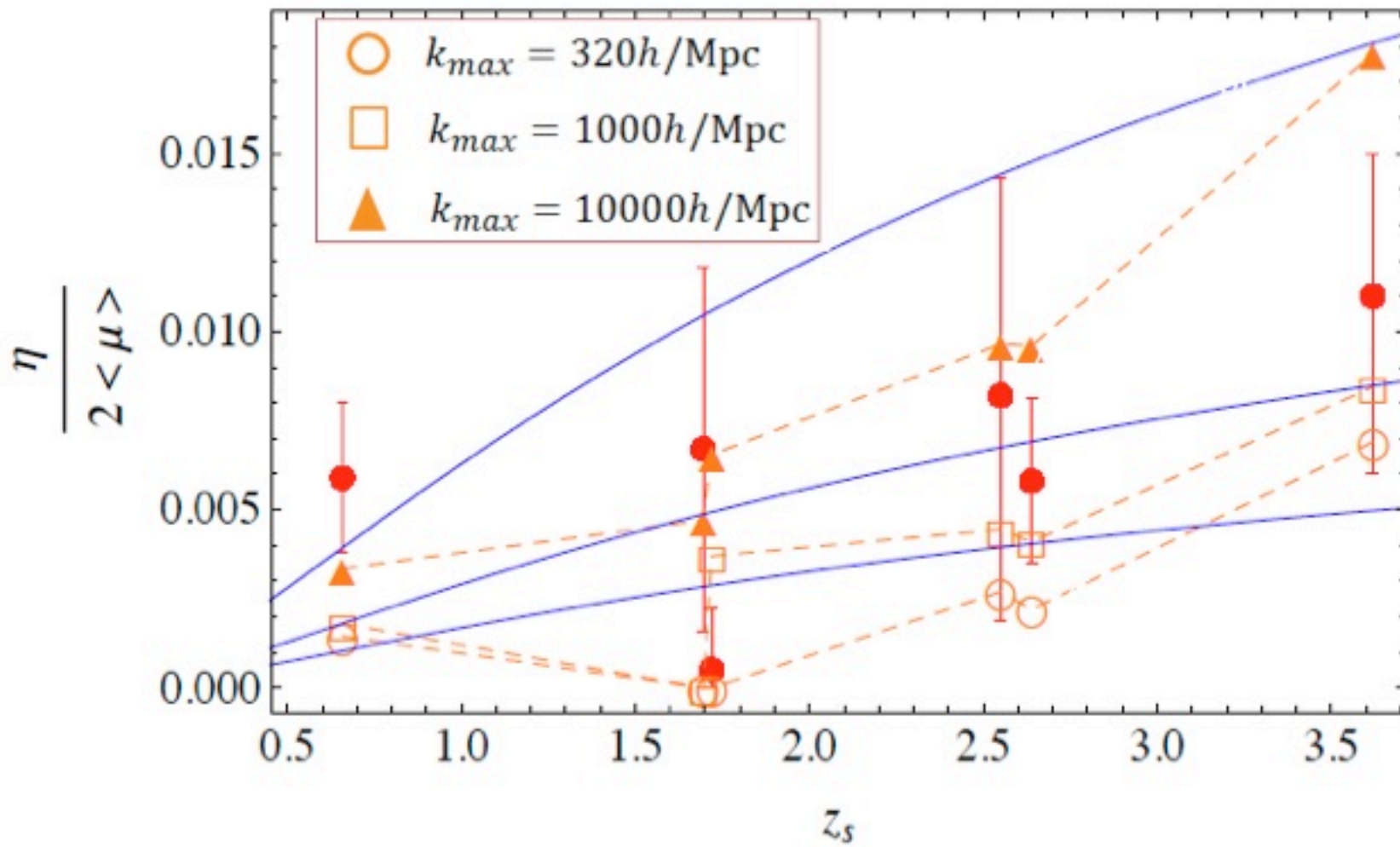
References: 1. CASTLES; 2. Sugai et al. 2007; 3. Minezaki et al. 2009; 4. Chiba et al. 2005; 5. MacLeod et al. 2009

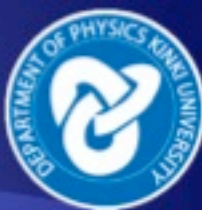
Note: (*): [OIII] line flux ratios. (**): The lens redshift z_L is obtained from a best-fit model using the observed positions of the images and the primary lens, the flux ratios, and the time-delays between the images assuming $H_0 = 70 \text{ km/s/Mpc}$.

Result I



Result II





Summary

- Clustering line-of-sight halos with $M=10^{3-7}$ solar mass can explain the observed anomalous flux ratios without any substructures inside a lensing galaxy.
- The estimated amplitudes of convergence perturbation increase with the source redshift as predicted by theoretical models.
- Unique probe into mini-halos $M<10^6$ solar mass



Future work

- Consistency check using light-ray tracing simulations
- Minimum change in astrometric shift for lensed image & lens.
- Check of SIE+ES, luminous group/satellite galaxies
- Extension to radio lenses incorporating finite source-size effects

